forests

MDPI

Article

Exploring the Relationship Between Forest Landscape Pattern and Seasonal Land Surface Temperature in Ningbo Using Extra Trees and SHAP

Lihao Zheng [1,2], Hao Yang [1,2,*], Hao Zeng [1,2] and Youbing Zhao [3]

[1] School of Media Engineering, Communication University of Zhejiang, Hangzhou 310018, China; 19990205@cuz.edu.cn (L.Z.); hao.zeng@cuz.edu.cn (H.Z.)
[2] National Radio and Television Administration Laboratory for Media Intelligent Communication Technology, Hangzhou 310018, China
[3] School of Computing, University of Derby, Derby DE22 1GB, UK; y.zhao@derby.ac.uk
* Correspondence: yanghao@cuz.edu.cn

Abstract

Urban forest landscape patterns play an important role in shaping the spatial heterogeneity of the land surface thermal environment, although their effects and associated response relationships may vary substantially across seasons. To investigate the complex relationships between forest landscape patterns and seasonal land surface temperature (LST), this study focused on Ningbo, China. Landsat 8 satellite imagery and the China Land Cover Dataset (CLCD) were used to derive LST and forest spatial distribution data for the period from March 2025 to February 2026. Given its ability to capture complex nonlinear relationships through an ensemble of randomized decision trees without requiring predefined functional forms, the Extra Trees algorithm was employed to develop separate seasonal models using seven forest landscape metrics. The SHapley Additive exPlanations (SHAP) method was further applied to quantify the relative contributions of individual metrics and elucidate their effects and nonlinear response patterns. The results revealed the following: (1) LST in Ningbo exhibited pronounced seasonal variations and spatial heterogeneity, with the highest values in summer and the lowest in winter. (2) The Extra Trees models demonstrated satisfactory predictive performance, with the winter model achieving the best overall performance, whereas the summer model exhibited relatively higher prediction errors. (3) The largest patch index (LPI) and landscape division index (DIVISION) were the two most influential landscape metrics across all four seasons. Specifically, LPI made relatively greater contributions in spring and summer, whereas DIVISION played a more dominant role in autumn and winter. (4) SHAP dependence analysis further revealed nonlinear and season-dependent relationships between forest landscape metrics and LST. LPI generally exhibited negative contributions, although its response patterns varied across seasons, showing a predominantly monotonic negative relationship in summer and non-monotonic patterns in autumn and winter. In contrast, DIVISION exhibited a relatively consistent nonlinear positive response across all four seasons. Furthermore, the directions and magnitudes of the effects of patch density (PD) and mean patch area (MPA) on model predictions varied seasonally. This study establishes an interpretable machine learning framework integrating Extra Trees and SHAP, providing quantitative insights into the identification of key urban forest landscape characteristics, the optimization of forest spatial configurations, and the development of season strategies for urban thermal environment regulation.

Academic Editor: Lei Wang

Received: 22 October 2026
Revised: 24 November 2026
Accepted: 25 November 2026
Published: 27 November 2026

Copyright: © 2026 by the authors. Licensee MDPI, Basel, Switzerland. This article is an open access article distributed under the terms and conditions of the Creative Commons Attribution (CC BY) license.

Keywords: urban forests; landscape patterns; land surface temperature; Extra Trees; SHAP; seasonal variations

1. Introduction

Against the backdrop of ongoing global climate change and accelerating urbanization, urban thermal environment issues have become increasingly pronounced, posing substantial challenges to urban ecological security, public health, and sustainable development [1,2]. Land surface temperature (LST) is a fundamental indicator of surface thermal conditions and the spatial heterogeneity of urban thermal environments, with important implications for the urban heat island effect, ecosystem functioning, and human thermal comfort [3,4]. Urban expansion has substantially transformed natural land cover and altered surface energy exchange processes. In particular, the expansion of impervious surfaces modifies surface radiative properties, heat storage, and evapotranspiration processes, thereby intensifying thermal stress in urban areas [5]. The increasing frequency and intensity of extreme heat events further underscore the urgency of effective urban thermal regulation. Accordingly, identifying the key determinants of LST and elucidating the thermal regulation mechanisms of urban natural ecosystems are essential for optimizing urban spatial configurations, mitigating heat-related risks, and strengthening urban climate resilience.

Urban forests constitute a fundamental component of urban green infrastructure and play an essential role in improving environmental quality and mitigating urban heat island effects [6,7]. Their cooling effects are primarily mediated through canopy shading and evapotranspiration, which reduce surface solar radiation absorption and facilitate the partitioning of available energy from sensible heat into latent heat [8,9]. In addition, urban forests modify surface aerodynamic roughness, local airflow patterns, and land–atmosphere water and energy exchanges, further contributing to thermal regulation [10,11]. Importantly, the cooling capacity of urban forests is determined not merely by their total area or vegetation coverage but also by their spatial configuration, patch morphology, fragmentation, and aggregation characteristics [12,13]. Variations in forest landscape organization can modify within patch microclimatic conditions, edge effects, and energy exchanges between forest patches and adjacent land covers, resulting in heterogeneous thermal responses. Consequently, investigating the relationships between forest landscape patterns and LST through an integrated framework combining landscape ecology and urban climatology can advance our understanding of the thermal regulation functions of urban forests and provide a scientific foundation for the spatial optimization of urban green infrastructure.

The effects of forest landscape patterns on LST are inherently complex and spatially heterogeneous, reflecting the combined influences of landscape composition, configuration, and connectivity. Forest patch size and spatial distribution influence vegetation coverage and landscape connectivity, while larger and more spatially aggregated patches generally provide more extensive interior habitats that support canopy shading and evapotranspiration [14]. Meanwhile, variations in patch shape complexity, edge characteristics, and fragmentation can modify material and energy exchanges between forest interiors and surrounding land covers, thereby affecting local thermal conditions. Landscape connectivity may further influence the ecological functionality of forest systems by shaping the structural continuity and spatial organization of urban green spaces [15]. Previous studies have demonstrated significant associations between LST and various forest landscape attributes, including patch area, morphological complexity, and spatial aggregation. Nevertheless, the relative importance and thermal effects of these attributes may differ

substantially across urban landscapes and environmental settings [16]. Thus, assessments based solely on forest area or vegetation coverage are insufficient to capture the multidimensional effects of forest spatial organization on the urban thermal environment. A comprehensive evaluation of forest landscape patterns is therefore necessary to disentangle the contributions of different landscape attributes to LST variations.

Furthermore, the thermal regulation effects of urban forests are subject to pronounced seasonal variations. Seasonal fluctuations in solar radiation, air temperature, precipitation, and soil moisture influence vegetation phenology, canopy development, and transpiration capacity, potentially modifying the relationships between forest landscape patterns and LST [17,18]. During the growing season, particularly in summer, vigorous vegetation growth and enhanced evapotranspiration may strengthen forest cooling effects. In contrast, reduced physiological activity and changes in canopy conditions during winter may alter the dominant thermal regulation processes. Previous research has demonstrated that the effects of urban green space morphology and vegetation composition on LST vary across seasons. However, the relative contributions of individual forest landscape attributes and their seasonal variations across spring, summer, autumn, and winter remain insufficiently understood. This knowledge gap limits a comprehensive understanding of how forest spatial configurations regulate urban thermal environments under varying seasonal conditions. Therefore, systematically comparing the relationships between forest landscape patterns and LST across the four seasons is essential for identifying season-dependent thermal regulation mechanisms and informing seasonally adaptive urban forest planning and management.

In recent years, machine learning has emerged as a powerful analytical approach for investigating the complex relationships between urban landscape patterns and LST [19,20]. Conventional statistical approaches predominantly rely on predefined functional relationships and often have limited capacity to capture the nonlinear interactions and complex dependencies among multiple landscape variables [21,22]. In contrast, ensemble learning algorithms can accommodate high dimensional predictors and characterize complex nonlinear relationships without imposing strict assumptions about data distributions. Among these algorithms, Extra Trees employ randomized feature selection and split point determination to construct an ensemble of decision trees, enabling robust modeling of complex relationships between landscape attributes and LST [23,24]. Nevertheless, despite their predictive capabilities, tree-based ensemble models are often regarded as black box approaches because their internal decision-making processes are difficult to interpret. To address this limitation, SHapley Additive exPlanations (SHAP), grounded in Shapley values from cooperative game theory, decompose individual model predictions into feature specific contributions. This approach quantifies the relative importance of explanatory variables while elucidating their contribution directions and nonlinear relationships with model outputs [25,26]. Recent studies have employed interpretable machine learning frameworks to identify the nonlinear effects of urban spatial morphology and landscape patterns on LST, offering new insights into the complex mechanisms underlying urban thermal environments [27]. Accordingly, integrating Extra Trees with SHAP provides a complementary framework that combines predictive capability with model interpretability, facilitating a more comprehensive understanding of the relationships between forest landscape patterns and seasonal LST.

Despite substantial progress in understanding the thermal regulation effects of urban forests, several important knowledge gaps remain. First, the relative contributions of different forest landscape attributes to LST and the extent to which their combined spatial configurations influence the thermal environment have not been sufficiently clarified. Second, the nonlinear relationships and potential threshold effects between forest landscape metrics and LST require further investigation. Third, the extent to which the relative importance and thermal

effects of individual forest landscape attributes vary across seasons remains insufficiently understood. To address these gaps, this study selects Ningbo City, China, as its study area and integrates Landsat satellite imagery with forest landscape metrics to establish an analytical framework based on Extra Trees and SHAP for investigating the relationships between urban forest landscape patterns and LST across the four seasons. Specifically, this study aims to (1) characterize the spatial distribution of LST in Ningbo during spring, summer, autumn, and winter; (2) employ the Extra Trees model to quantify the relative importance of different forest landscape attributes in explaining seasonal LST variations; and (3) utilize SHAP analysis to elucidate the contribution directions and nonlinear response patterns of key forest landscape attributes, identify potential response thresholds, and compare their thermal environmental effects across seasons. By addressing these objectives, this study seeks to advance the understanding of the relationships between urban forest landscape configuration and seasonal thermal environments, providing scientific support for urban forest spatial optimization, ecological resource management, and climate adaptive planning strategies to mitigate heat related risks.

2. Materials and Methods

2.1. Study Area

Ningbo lies in northeastern Zhejiang Province, on the southern flank of the Yangtze River Delta along the East China Sea. Its landscape comprises a mosaic of coastal plains, river networks, and hilly and mountainous terrain. This study focuses on six administrative districts, namely Haishu, Jiangbei, Zhenhai, Beilun, Yinzhou, and Fenghua (Figure 1). Variations in topography and urban development intensity contribute to considerable spatial heterogeneity in forest distribution. Forest patches differ in size, shape, aggregation, and connectivity, providing a suitable setting for investigating the relationships between forest landscape patterns and LST.

Ningbo has a subtropical monsoon climate characterized by four distinct seasons and pronounced seasonal variations in meteorological conditions. Spring is marked by rising temperatures and increasing precipitation, whereas summer features high temperatures, concentrated rainfall, and intense solar radiation. Autumn brings progressively cooler conditions, while winter is characterized by low temperatures and reduced vegetation physiological activity. Seasonal changes in solar radiation, hydrothermal conditions, and vegetation growth may influence LST and its spatial distribution by modifying canopy shading and evapotranspiration.

Ongoing urbanization, together with the expansion of built-up areas and changes in forest landscape patterns, may further alter the urban thermal environment through changes in surface energy exchange. Accordingly, investigating the nonlinear relationships between forest landscape patterns and seasonal LST, together with their seasonal variations, can improve understanding of the thermal regulation functions of urban forests. The findings may also provide a scientific basis for optimizing forest spatial configurations, mitigating urban thermal stress, and enhancing ecosystem services in Ningbo.

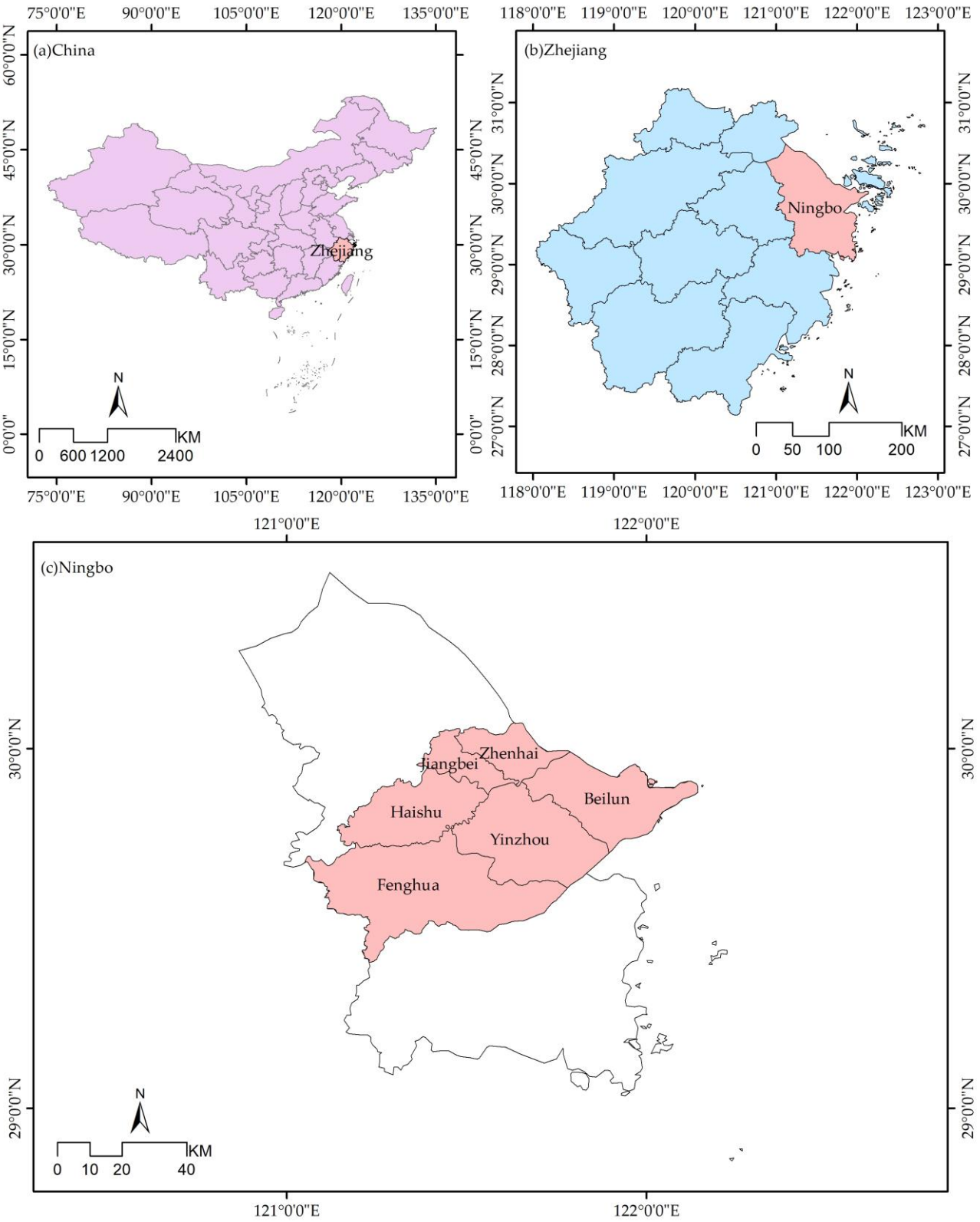


Figure 1. Map of the study area.

2.2. Data Sources

This study employed the Landsat 8 Collection 2 Level-2 Land Surface Temperature product provided by the United States Geological Survey (USGS), with the corresponding remote sensing data accessed through the Google Earth Engine (GEE) platform [28]. The product includes a surface temperature band (ST_B10), whose pixel values are encoded using a scale factor and an additive offset. These values were converted into actual land

surface temperature (LST) values according to the official USGS product specifications. To systematically characterize seasonal variations in LST across the study area, Landsat 8 imagery acquired during the four seasons was selected, and a 2025 land cover mask was applied to ensure spatial consistency in LST extraction across seasons. Accordingly, four seasonal LST datasets were generated for spring, summer, autumn, and winter. Following the meteorological definition of seasons, spring was defined as March–May 2025, summer as June–August 2025, autumn as September–November 2025, and winter as December 2025–February 2026.

Forest spatial distribution data for the study area were derived from the China Land Cover Dataset (CLCD), which was developed using Landsat satellite imagery and provides long-term land cover records at a spatial resolution of 30 m. The dataset enables the identification of major land cover types, including forests, croplands, grasslands, water bodies, and impervious surfaces, and has been widely used in land cover change detection, ecological and environmental assessments, and landscape pattern analysis. In this study, forest-class pixels were extracted from the 2025 CLCD to generate a spatially explicit forest distribution dataset for the study area. The extracted data were subsequently clipped to the study area boundary, projected into a common coordinate reference system, and spatially aligned with the Landsat 8 land surface temperature data to ensure consistency in spatial reference and analytical extent. Based on the processed forest distribution data, forest landscape pattern indices were calculated to provide quantitative indicators for examining the relationships between forest landscape patterns and seasonal LST.

2.3. Methods

The methodological framework of this study (Figure 2) consists of four sequential and interrelated steps designed to systematically investigate the relationships between urban forest landscape patterns and seasonal LST, with particular emphasis on quantifying the relative contributions of different forest landscape attributes and identifying their nonlinear response patterns.

(1) Seasonal LST retrieval and characterization of the thermal environment. Landsat 8 satellite imagery was processed using the GEE platform to derive LST datasets for the four seasons: spring, summer, autumn, and winter. The resulting seasonal datasets were used to characterize the spatiotemporal distribution of LST and identify seasonal variations in the thermal environment across the study area. This step provides the fundamental thermal information required for subsequent investigations into the relationships between forest landscape patterns and seasonal LST.

(2) Extraction of forest spatial distribution and quantification of landscape patterns. Forest distribution across the study area was extracted from the CLCD, and seven representative landscape metrics were selected to establish a forest landscape indicator system. These metrics were used to translate the spatial characteristics of forest landscapes into quantitative explanatory variables, capturing their compositional and configurational attributes. This step provides the landscape predictors required to assess the relationships between forest spatial structure and LST.

(3) Modeling the relationships between forest landscape patterns and LST. Forest landscape metrics were spatially matched with the corresponding seasonal LST datasets to construct a sample database based on consistent spatial analysis units, ensuring spatial correspondence between the explanatory and response variables. Subsequently, the Extra Trees algorithm was employed to model the complex relationships between forest landscape attributes and LST, accounting for potential nonlinear associations and interactions among predictors. This step aims to overcome the limitations of conventional linear approaches in representing complex variable relationships and to evaluate the relative importance of different forest landscape attributes in explaining seasonal LST variations.

https://doi.org/10.3390/f17121444

(4) Model interpretation and identification of nonlinear response patterns. The SHAP framework was employed to interpret the Extra Trees model predictions from the perspectives of feature importance and feature-response relationships. SHAP feature importance analysis was used to quantify the relative contributions of individual landscape metrics to model predictions. Furthermore, the distribution and variation in SHAP values were examined to determine the direction and magnitude of feature contributions and characterize nonlinear response patterns between forest landscape attributes and LST. This step enhances the interpretability of the machine learning framework, facilitates comparisons of the relationships between individual forest landscape attributes and seasonal LST, and provides scientific insights into urban forest spatial optimization and thermal environment regulation.

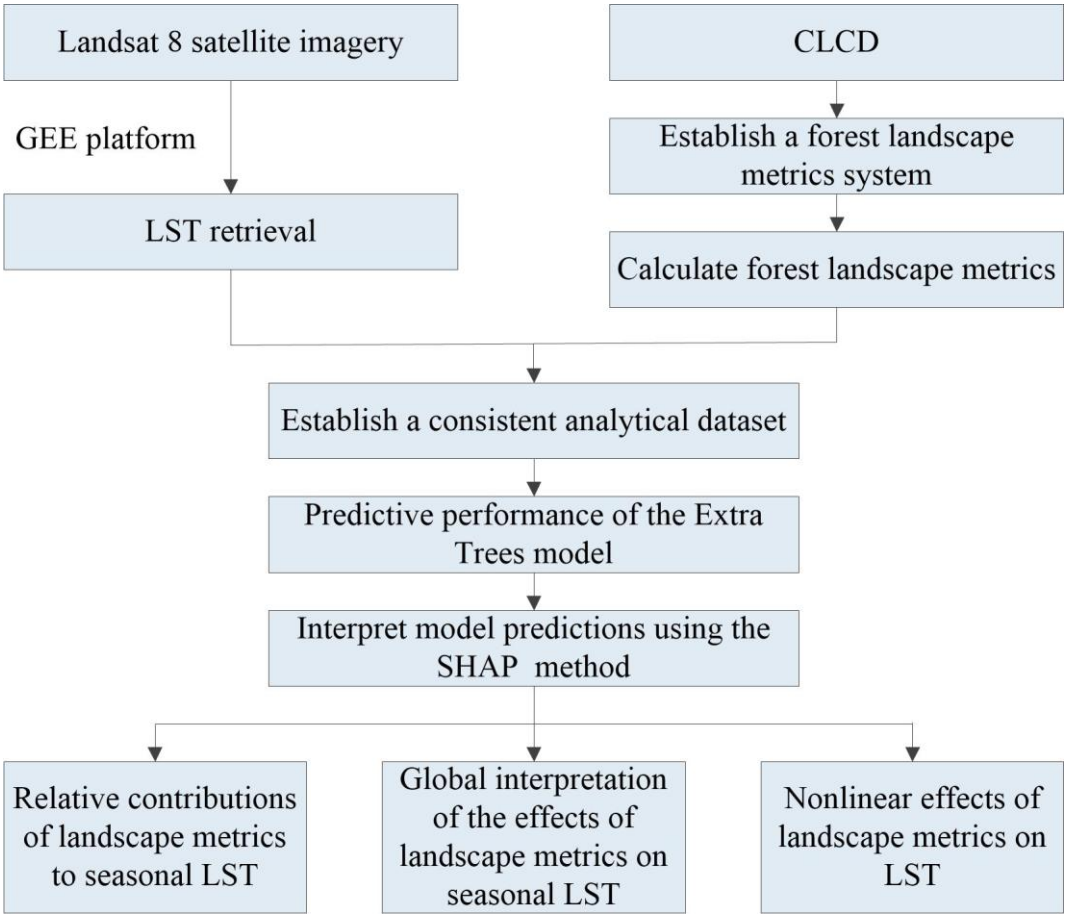


Figure 2. Methodological framework of this study.

2.3.1. LST Retrieval

LST was derived from the ST_B10 band of the Landsat 8 Collection 2 Level-2 surface temperature product [29]. As the USGS product provides atmospherically corrected surface temperature estimates derived from thermal infrared observations and relevant atmospheric and surface parameters, no additional thermal infrared radiative transfer inversion was performed. Instead, the original pixel values were converted to physical temperatures using the scale factor and additive offset specified in the product documentation, and the resulting temperatures in Kelvin were converted to degrees Celsius. The LST calculation is expressed as follows:

$$\mathrm{LST} = (0.00341802 \times \mathrm{ST}_{\mathrm{B10}} + 149.0) - 273.15 \quad (1)$$

where LST denotes land surface temperature (°C), and ST_{B10} represents the original pixel values of the surface temperature band in the Landsat 8 Collection 2 Level-2 product. The scaling factor (0.00341802) and additive offset (149.0) are applied to convert the original stored values to temperature in Kelvin, which is then converted to degrees Celsius by subtracting 273.15. These parameters were obtained from the official USGS product specifications.

Landsat 8 satellite imagery covering the study area during the four seasons of 2025 was initially acquired and filtered using the GEE platform according to the spatial extent of the study area and the corresponding seasonal time windows. The pixel quality assessment band (QA_PIXEL) was subsequently employed to mask clouds, cloud shadows, and other invalid observations, thereby improving the reliability of the retrieved surface temperature data. The surface temperature band (ST_B10) was then converted into physical temperature values using the scaling factor and additive offset specified in the USGS product documentation, with temperatures expressed in degrees Celsius (°C). Finally, pixel-wise median compositing was performed on the valid observations for each season (spring, summer, autumn, and winter) to minimize the influence of residual outliers and random observational errors on seasonal LST estimates. This procedure generated four seasonal LST raster datasets for the study area, providing a consistent basis for subsequent spatial analysis.

2.3.2. Forest Landscape Metrics

To quantitatively characterize the spatial structure and morphological characteristics of urban forest landscapes, seven representative landscape pattern metrics were selected to establish a forest landscape metric system (Table 1), and their values were calculated using FRAGSTATS 4.2. Based on the study area boundaries, a regular grid with a cell size of 600 × 600 m was generated using a consistent projected coordinate reference system, with each grid cell serving as a standardized spatial analysis unit. A total of 11,975 grid cells were generated, of which 8016 contained forest cover and were therefore retained as valid forest grid cells. For grid cells intersecting the study area boundaries, spatial clipping was performed to exclude areas outside the study area, and only the portions within the study area were retained for subsequent analyses. Grid cells without forest cover were excluded from forest landscape metric calculations and subsequent model analyses.

To ensure spatial consistency across seasons, all seasonal LST rasters, land cover datasets, and landscape metrics were processed using a common spatial reference system, spatial extent, and pixel alignment. Where datasets differed in spatial resolution, appropriate resampling methods were applied according to data type: bilinear interpolation was used for continuous variables, whereas nearest-neighbor resampling was applied to categorical data. Missing or invalid pixels were identified and excluded based on quality control procedures, and missing LST values were not artificially imputed. Only grid cells satisfying the data validity criteria for the corresponding season were retained for subsequent model analyses.

Forest landscape metrics were calculated using FRAGSTATS 4.2 at the class level, with the eight-neighbor (Queen's case) rule adopted to define patch connectivity and adjacency. Under this rule, forest pixels sharing either an edge or a corner were considered spatially connected and assigned to the same patch. Forest landscape metrics were extracted for each grid cell, and the mean LST for each corresponding grid cell was calculated separately for spring, summer, autumn, and winter. This standardized grid framework enabled the spatially consistent integration of forest landscape characteristics and seasonal LST, providing a common basis for subsequent statistical analyses and machine learning modeling.

Table 1. Description of forest landscape metrics.

Metrics	Abbreviation	Description
Largest Patch Index	LPI	Measures the area of the largest forest patch as a percentage of the entire analysis unit, highlighting the prominence of the dominant patch.
Mean Patch Area	MPA	Calculates the average size of individual forest patches, providing an indication of the typical spatial extent of forest fragments.
Mean Shape Index	MSI	Evaluates the average irregularity of forest patch boundaries relative to standard geometric shapes, reflecting morphological variation.
Landscape Shape Index	LSI	Assesses the complexity of the overall forest landscape configuration by comparing actual patch perimeter with the perimeter of an equivalent compact arrangement.
Edge Density	ED	Quantifies forest boundary length per unit of landscape area, characterizing the intensity of edge formation across the study area.
Patch Density	PD	Expresses the number of forest patches relative to the total landscape area, providing a measure of patch distribution and spatial subdivision.
Landscape Division Index	DIVISION	Assesses the extent of forest landscape separation by estimating the likelihood that two randomly chosen locations fall within different forest patches.

2.3.3. Extra Trees Modeling

This study employed the Extra Trees algorithm to develop predictive models linking forest landscape metrics to seasonal LST, with the aim of characterizing their complex nonlinear relationships. Although satellite remote sensing provides essential information on forest spatial distribution and surface thermal conditions, remote sensing data alone cannot fully elucidate the complex relationships between forest landscape characteristics and LST. Accordingly, machine learning techniques were introduced to establish quantitative relationships between forest landscape patterns and LST, thereby identifying potential associations between individual landscape attributes and the urban thermal environment.

Extra Trees is an ensemble learning algorithm based on decision trees that incorporates randomization into the feature selection and split point determination processes to construct a diverse ensemble of decision trees. The predictions generated by individual trees are subsequently aggregated to enhance the model's predictive capability and generalization performance. Unlike Random Forests [30], which typically identify optimal split points from randomly selected candidate features, Extra Trees introduces additional randomness by generating candidate splitting thresholds randomly and selecting the optimal split from these candidates. This additional randomization increases the diversity among individual trees and can help reduce prediction variance and improve model robustness. Furthermore, unlike conventional linear regression approaches [31], Extra Trees does not require predefined functional relationships between predictors and response variables, enabling it to capture complex nonlinear associations and interactions among explanatory variables. These characteristics make Extra Trees particularly suitable for modeling the relationships between forest landscape metrics and LST, providing a quantitative basis for assessing the relative importance of different landscape attributes and their associations with seasonal thermal variations.

Seven forest landscape metrics were used as predictor variables, while the LST of the corresponding spatial analysis units served as the response variable. Separate Extra Trees models were developed for spring, summer, autumn, and winter to investigate seasonal variations in the relationships between forest landscape patterns and LST. To evaluate model predictive performance, the dataset was randomly partitioned into training and testing sets at a ratio of 8:2, with 80% of the samples allocated for model training and the

remaining 20% reserved for independent testing. This random partitioning strategy enables the assessment of model performance on samples not used during training. However, given the spatial nature of the study data, geographically proximate samples may share similar environmental characteristics and LST values, resulting in spatial autocorrelation. Consequently, random partitioning may distribute spatially adjacent samples across both the training and testing sets, thereby introducing spatial dependence between the two subsets and compromising the spatial independence of the testing set. Such spatial dependence may lead to overly optimistic estimates of predictive performance, as the model may be evaluated on testing samples that exhibit strong spatial similarity to those in the training set. Five-fold cross-validation was implemented during model training to assess model stability and reduce the potential for overfitting, while the independent testing set was used to evaluate predictive performance on unseen samples. To ensure consistency and comparability across seasons, identical hyperparameter settings were adopted for all four models. Specifically, the number of trees (n_estimators) was set to 100, the maximum tree depth (max_depth) to 10, the minimum number of samples required to split an internal node (min_samples_split) to 2, and the minimum number of samples required at a leaf node (min_samples_leaf) to 1. The random seed (random_state) was fixed at 42 to ensure the reproducibility of the model training process.

Model performance was evaluated using the root mean square error (RMSE), mean absolute error (MAE), and coefficient of determination (R^2). RMSE measures the magnitude of prediction errors and assigns greater weight to larger deviations between predicted and observed values. MAE represents the average absolute prediction error, providing an intuitive measure of prediction accuracy. R^2 quantifies the proportion of variance in observed LST explained by the model. Lower RMSE and MAE values indicate smaller prediction errors, whereas an R^2 value closer to 1 generally indicates greater explanatory performance. By comparing these evaluation metrics across the four seasonal models, this study assessed the capability of Extra Trees to characterize the relationships between forest landscape patterns and seasonal LST. The optimized models were subsequently used as the basis for SHAP analysis to quantify the contributions of individual landscape metrics to model predictions, determine their contribution directions, and identify potential nonlinear response patterns.

2.3.4. SHAP Model Interpretation Method

To elucidate the nonlinear relationships between forest landscape metrics and seasonal LST, as well as their seasonal variations, the SHAP framework was employed to interpret the Extra Trees models. Grounded in Shapley values from cooperative game theory, SHAP decomposes individual model predictions into feature-specific contributions, thereby quantifying the relative importance of forest landscape metrics and revealing their contribution directions and response patterns.

In this study, three complementary SHAP visualization techniques, namely bar plots, summary plots, and dependence plots, were integrated to examine model interpretability from the perspectives of feature importance, contribution distributions, and nonlinear response characteristics. First, SHAP bar plots were generated using the mean absolute SHAP value of each forest landscape metric to quantify and rank its overall contribution to model predictions. Larger mean absolute SHAP values indicate greater relative importance in the model's predictive output. Second, SHAP summary plots were employed to characterize the distribution of SHAP values and their associations with corresponding feature values. Positive SHAP values indicate that a given feature contributes to an increase in the predicted LST relative to the model's baseline prediction, whereas negative values indicate a contribution toward lower predicted LST. The color gradient, ranging from blue to red, represents increasing feature values and provides additional insight into

how variations in landscape metrics are associated with changes in model predictions. Finally, SHAP dependence plots were used to investigate the nonlinear response relationships between individual forest landscape metrics and model-predicted LST. In these plots, feature values are represented on the x-axis, while their corresponding SHAP values are displayed on the y-axis, enabling the identification of contribution directions, response magnitudes, and potential transition points along the feature-value range. By applying these three SHAP visualization approaches to the four seasonal models (spring, summer, autumn, and winter), we systematically compared the relative importance rankings, contribution distributions, and nonlinear response patterns of forest landscape metrics across seasons, thereby identifying seasonal differences in their associations with LST. It should be emphasized that SHAP values quantify the contributions of individual features to model predictions and should not be interpreted as evidence of direct causal relationships between variables.

3. Results

3.1. Spatial Distribution Characteristics of Seasonal LST

LST across the study area exhibited pronounced seasonal variations and considerable spatial heterogeneity (Figure 3). The mean LST values in spring, summer, autumn, and winter were 22.74, 38.76, 26.42, and 13.22 °C, respectively, indicating a clear seasonal pattern, with the highest temperatures occurring in summer, followed by autumn and spring, and the lowest in winter.

The spatial distribution of LST also varied substantially across seasons. In spring, LST generally exhibited a spatial pattern characterized by relatively high temperatures in the central and northern regions and lower temperatures in the southern and southwestern regions. High temperature areas were primarily concentrated in the central and northern parts of the study area, particularly in densely urbanized zones, where they formed fragmented patches and elongated belts. By contrast, relatively low temperatures prevailed in localized areas in the south, southwest, and southeast, forming comparatively continuous low temperature patches. During summer, high temperature areas expanded considerably, accompanied by a more pronounced spatial temperature gradient. Relatively concentrated high temperature clusters emerged in the central and northern regions, as well as in areas characterized by intensive transportation infrastructure and construction activities. Meanwhile, parts of the southern, southwestern, and eastern regions remained relatively cool, indicating more pronounced spatial differentiation in summer LST. In autumn, high temperature areas contracted to some extent compared with summer, although the central and northern regions continued to exhibit relatively elevated temperatures. Moderate to low temperatures predominated in parts of the western, southern, and southeastern regions, resulting in a spatial distribution pattern broadly comparable to that observed in spring. In winter, LST decreased substantially across the study area. Relatively high temperatures were mainly concentrated in the central and northern regions and in localized urbanized areas, whereas lower temperatures dominated parts of the southwestern, southern, and eastern regions. Despite the marked seasonal decline in overall temperature levels, distinct spatial differences in LST persisted throughout the study area.

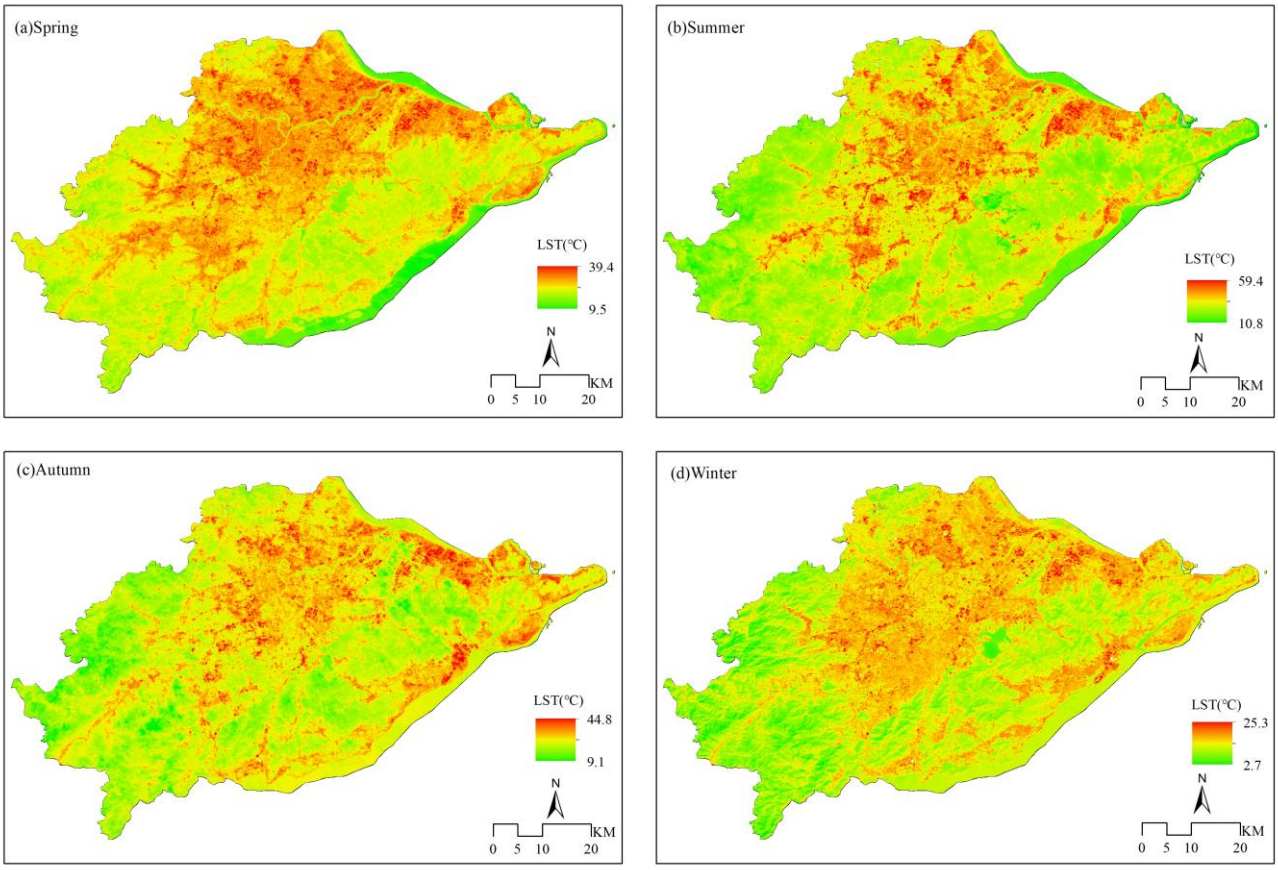


Figure 3. Spatial distribution of seasonal LST.

3.2. Predictive Performance of the Extra Trees Model

The predictive performance of the Extra Trees model exhibited distinct seasonal variations in estimating LST (Table 2). R^2 was highest in winter, followed by summer and autumn, whereas spring yielded the lowest value, indicating that the model provided the greatest explanatory power for the spatial variability of winter LST. Regarding prediction errors, the RMSE and MAE were 1.943 °C and 1.433 °C in spring, 2.896 °C and 2.158 °C in summer, and 2.218 °C and 1.742 °C in autumn, respectively. Winter exhibited the lowest prediction errors, with an RMSE of 1.195 °C and an MAE of 0.913 °C. The Extra Trees model achieved its best predictive performance in winter, whereas its prediction errors were greatest in summer. These results highlight seasonal differences in the predictive performance of the model, potentially reflecting seasonal variations in the relationships between forest landscape patterns and LST.

Table 2. Model performance across the four seasons.

Season	RMSE (°C)	MAE (°C)	R^2
Spring	1.943	1.433	0.554
Summer	2.896	2.158	0.590
Autumn	2.218	1.742	0.585
Winter	1.195	0.913	0.634

3.3. Relative Contributions of Forest Landscape Metrics to Seasonal LST

The SHAP bar plots illustrate the relative contributions of forest landscape metrics to LST across the four seasons and reveal seasonal variations in their relative importance (Figure 4). The contributions of forest landscape metrics to LST exhibited pronounced seasonal heterogeneity. Among these metrics, the LPI and DIVISION consistently made substantial contributions in all four seasons, highlighting the importance of patch dominance and landscape fragmentation in explaining seasonal variations in LST. By contrast, PD, ED, and MSI generally exhibited relatively low contributions.

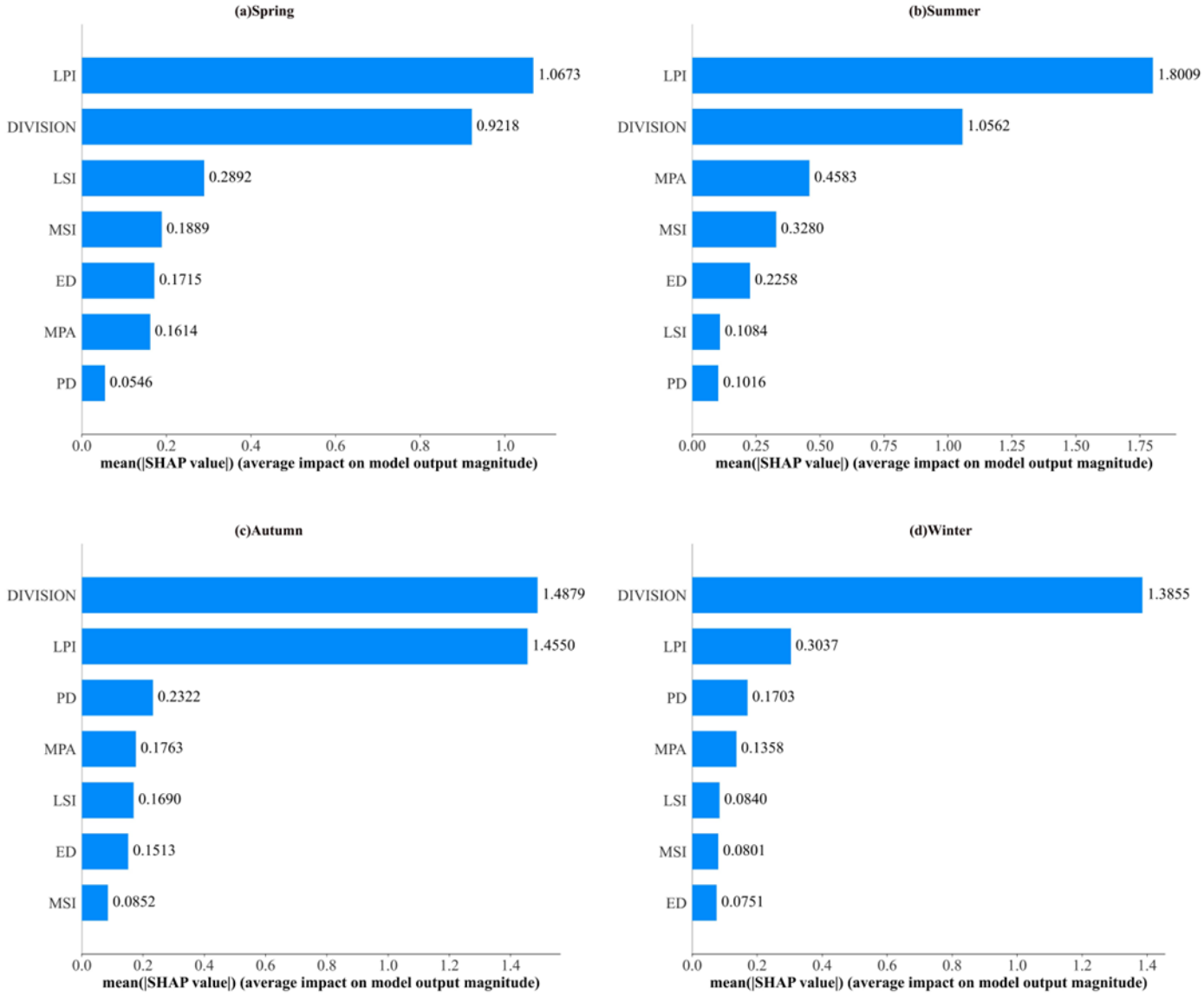


Figure 4. Relative contributions of forest landscape metrics to seasonal LST.

In spring, LPI made the greatest contribution, with a mean absolute SHAP value of 1.0673, followed by DIVISION. Both metrics contributed substantially more than the remaining indices. The LSI ranked third, while MSI, ED, and MPA exhibited comparable contributions. PD had the lowest contribution. In summer, the contribution of LPI increased to 1.8009, the highest value recorded for any metric across the four seasons, followed by DIVISION. MPA and MSI ranked third and fourth, respectively, whereas ED, LSI, and PD made relatively minor contributions. In autumn, the contribution of DIVISION increased to 1.4879, slightly exceeding that of LPI and making it the most influential

metric in this season. Among the remaining metrics, PD made the largest contribution, followed by MPA, LSI, and ED, while MSI had the lowest contribution. In winter, DIVISION remained the most influential metric, with a contribution substantially higher than that of LPI. PD and MPA ranked third and fourth, respectively, whereas LSI, MSI, and ED all exhibited relatively low contributions.

LPI and DIVISION were consistently the two most influential metrics across the four seasons, although their relative importance varied seasonally. LPI was the dominant contributor in spring and summer, whereas DIVISION ranked first in autumn and winter. The contribution of LPI peaked in summer, while the contributions of LPI and DIVISION were most similar in autumn. These findings demonstrate the seasonal variability in the relative contributions of forest landscape patterns to LST and identify patch dominance and landscape fragmentation as particularly important landscape characteristics for explaining spatial variations in LST across seasons.

3.4. Global Interpretation of the Effects of Forest Landscape Metrics on Seasonal LST

The SHAP summary plots further illustrate the direction, relative magnitude, and distribution of the contributions of individual forest landscape metrics to predicted LST across the four seasons (Figure 5). Positive and negative SHAP values indicate that a given metric increases or decreases the model predicted LST, respectively, relative to the model's baseline prediction. Larger absolute SHAP values indicate greater contributions to the model output. Feature values are represented by a color gradient from blue to red, corresponding to low to high metric values. Overall, the contributions of forest landscape metrics to LST exhibited pronounced seasonal heterogeneity. Notably, the LPI and DIVISION consistently ranked among the most important metrics across all four seasons and showed relatively stable contribution directions. LPI predominantly exhibited negative SHAP values, whereas DIVISION generally exhibited positive SHAP values. These patterns highlight the importance of dominant forest patch size and landscape fragmentation in explaining seasonal spatial variations in LST.

In spring, LPI and DIVISION exhibited contrasting contribution patterns. High LPI values were predominantly associated with negative SHAP values, whereas low LPI values were more frequently associated with positive SHAP values, suggesting that larger dominant forest patches tend to be associated with lower predicted LST. Conversely, high DIVISION values were mainly associated with positive SHAP values, indicating that greater landscape fragmentation tends to contribute to higher predicted LST. LSI generally exhibited positive SHAP values, whereas the SHAP values of MSI, ED, and MPA were largely concentrated around zero, suggesting relatively small contributions to model predictions. High PD values generally showed negative contributions, although this relationship exhibited some variability.

In summer, the contribution patterns of LPI and DIVISION became more pronounced. High LPI values were predominantly associated with larger negative SHAP values, suggesting a stronger negative contribution to predicted LST at higher levels of patch dominance. DIVISION exhibited the opposite pattern, with high values mainly corresponding to positive SHAP values. High MPA values were generally associated with negative SHAP values, indicating that larger average forest patch areas may contribute to lower predicted LST. By contrast, MSI and LSI predominantly exhibited positive contributions, suggesting that greater patch shape complexity was associated with higher predicted LST. ED generally showed negative contributions, whereas the SHAP values of PD were primarily concentrated around zero.

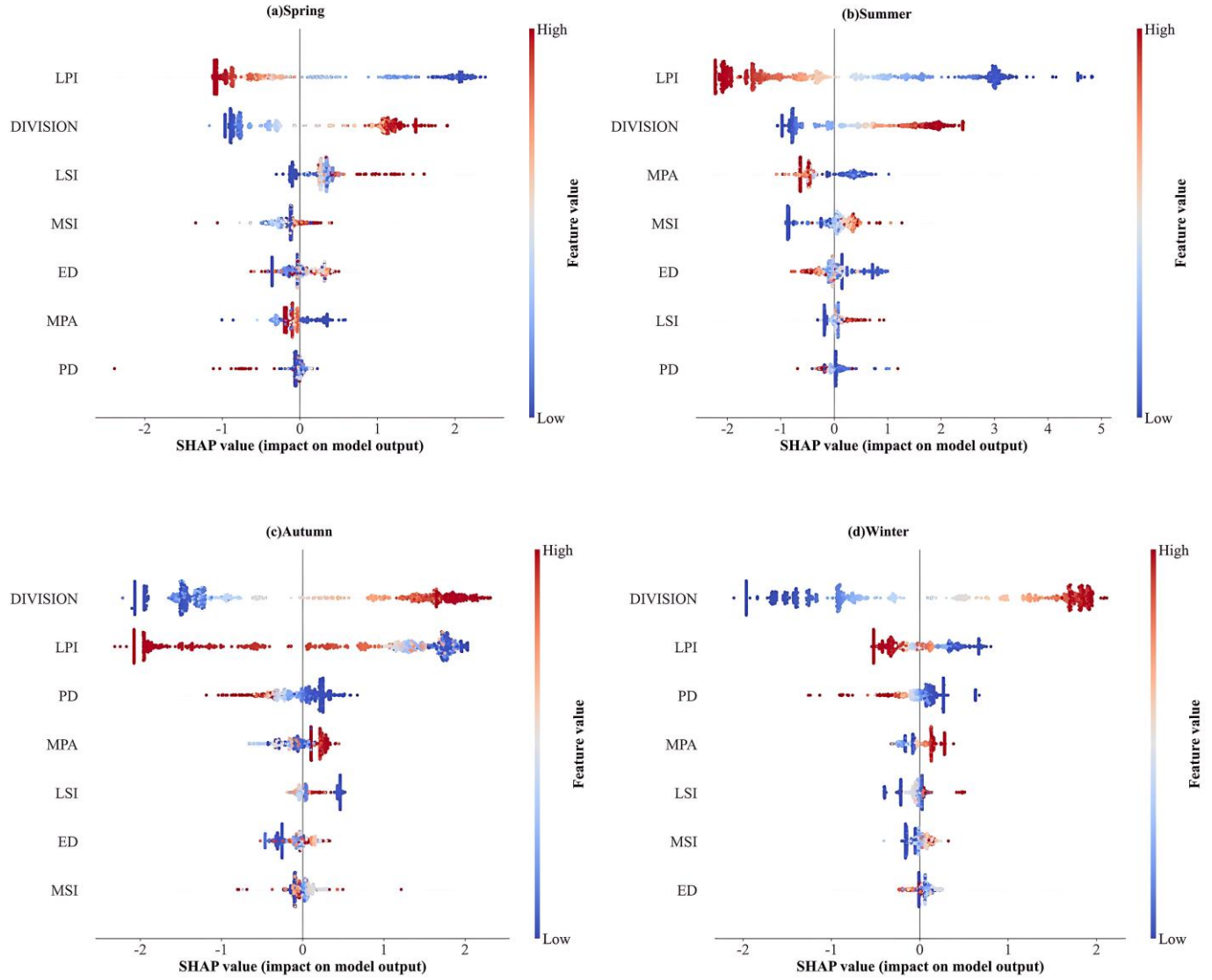


Figure 5. Global interpretation of the effects of forest landscape metrics on seasonal LST.

In autumn, DIVISION and LPI remained the two most influential metrics, with contribution directions broadly consistent with those observed in spring and summer. High DIVISION values were predominantly associated with positive SHAP values, whereas high LPI values were mainly associated with negative SHAP values. These patterns further suggest that greater landscape fragmentation is associated with higher predicted LST, while larger dominant forest patches tend to be associated with lower predicted LST. In addition, high PD values generally exhibited negative contributions, whereas high MPA values were primarily associated with positive SHAP values. The SHAP values of LSI, ED, and MSI were largely concentrated around zero, indicating comparatively limited contributions to model predictions.

In winter, DIVISION exhibited the strongest positive contribution, with high values predominantly corresponding to larger positive SHAP values, whereas low values were more frequently associated with negative SHAP values. LPI continued to exhibit a predominantly negative contribution, with high values mainly corresponding to negative SHAP values, suggesting an association between larger dominant forest patches and lower predicted LST. Furthermore, high PD values generally made negative contributions, whereas high MPA values were primarily associated with positive contributions. By comparison, MSI, ED, and LSI exhibited relatively limited contributions to the model predictions.

Taken together, the SHAP results reveal pronounced seasonal variations in the contributions of forest landscape metrics to LST, although LPI and DIVISION maintained relatively consistent contribution directions throughout the year. LPI predominantly exhibited negative contributions across all four seasons, whereas DIVISION generally showed positive contributions. These contrasting patterns highlight the different roles of dominant forest patch size and landscape fragmentation in explaining the spatial variation in the urban thermal environment. By comparison, the contribution directions and magnitudes of MPA, PD, LSI, and ED varied more substantially among seasons, with MPA showing particularly evident seasonal changes in its contribution direction. These findings indicate that the relationships between forest landscape patterns and LST are complex, nonlinear, and seasonally dependent.

3.5. Nonlinear Effects of Forest Landscape Metrics on LST

The SHAP dependence plots further reveal the nonlinear relationships between forest landscape metrics and seasonal LST, highlighting potential transition points in their contributions to model predictions (Figure 6). The relationships between individual landscape metrics and their SHAP values exhibited pronounced nonlinear characteristics, with the direction, magnitude, and response patterns varying across seasons.

In spring, LPI generally exhibited a negative relationship with its SHAP values. When LPI was below approximately 40, SHAP values were predominantly positive, indicating that lower LPI values generally made positive contributions to predicted LST. As LPI increased beyond approximately 50, SHAP values generally became negative, suggesting that higher LPI values increasingly contributed to lower predicted LST. DIVISION exhibited a distinct nonlinear positive response pattern. At values below approximately 0.45, SHAP values were predominantly negative. Between 0.45 and 0.60, SHAP values increased rapidly and generally became positive when DIVISION exceeded approximately 0.60. LSI generally made a positive contribution to predicted LST over the range of 1.0–2.0. At values above 2.0, however, SHAP values became substantially more dispersed, indicating greater variability in the metric's contributions to model predictions at higher LSI values.

In summer, LPI exhibited a relatively clear monotonic negative relationship with SHAP values. As LPI increased, SHAP values progressively declined from relatively high positive values and generally became negative within the range of approximately 50–60. This negative contribution became more pronounced when LPI exceeded 70. DIVISION displayed a pronounced nonlinear positive response, with SHAP values increasing rapidly over the range of approximately 0.20–0.50. This upward trend continued at higher DIVISION values, with SHAP values reaching relatively high levels as DIVISION approached 1.0. MPA generally exhibited a negative relationship with SHAP values. When MPA was below approximately 12, SHAP values were predominantly positive. As MPA increased beyond approximately 13, SHAP values gradually shifted toward negative values and remained relatively stable within the negative range at MPA values of approximately 20–40.

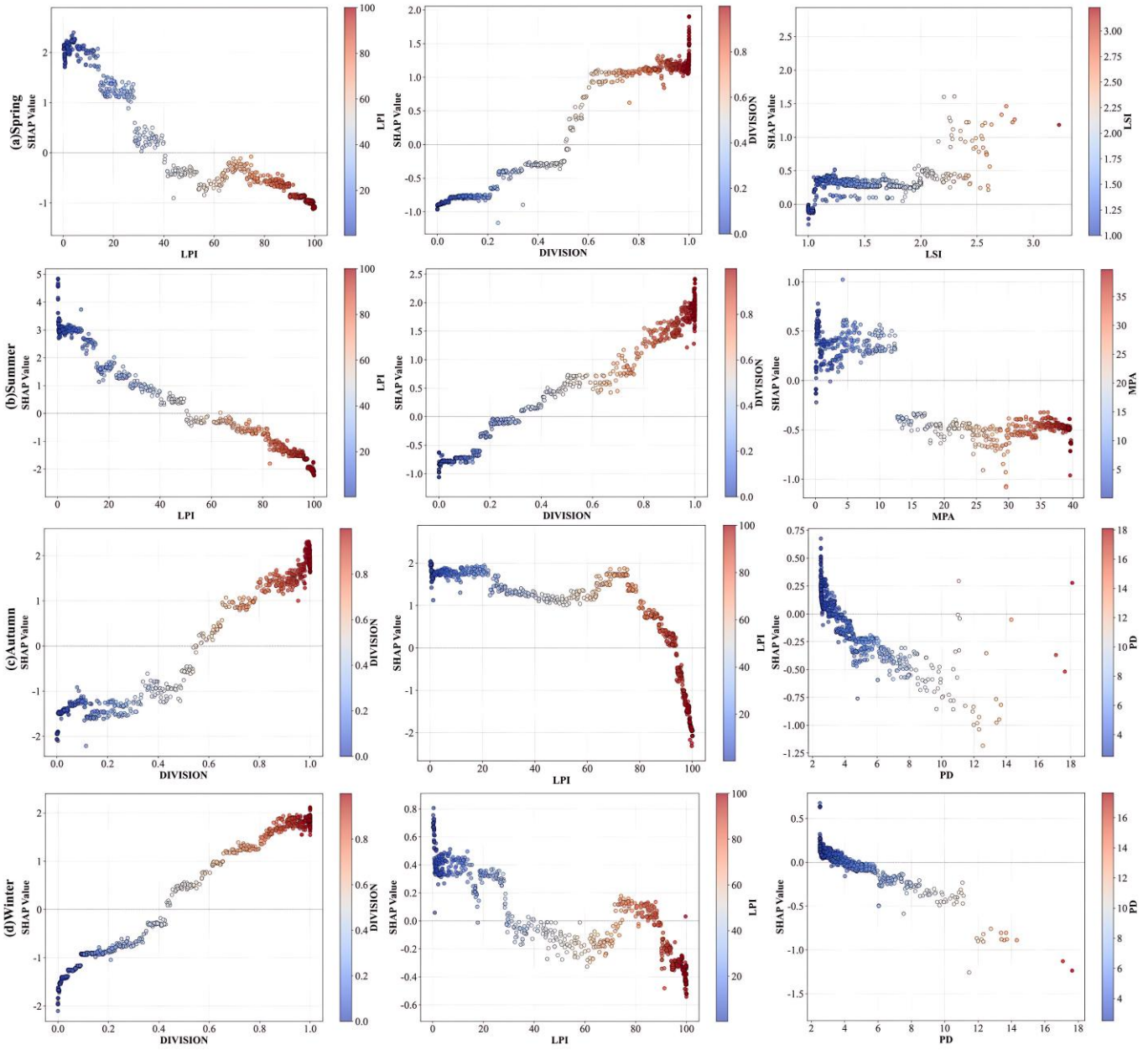


Figure 6. Nonlinear effects of forest landscape metrics on LST.

In autumn, DIVISION exhibited a pronounced S-shaped response pattern. At values below approximately 0.40, SHAP values were predominantly negative. Between approximately 0.45 and 0.65, SHAP values increased rapidly, transitioning from negative to positive around 0.55 and subsequently maintaining a relatively strong positive contribution. LPI exhibited a more complex, non-monotonic response. At relatively low LPI values, SHAP values remained strongly positive before gradually declining and stabilizing at comparatively low levels within the range of approximately 40–60. A moderate rebound occurred between 65 and 80, followed by a sharp decline when LPI exceeded approximately 85, resulting in predominantly negative contributions at higher values. PD generally exhibited a negative relationship with SHAP values, which progressively decreased as PD increased and transitioned from positive to negative around 4–5.

In winter, DIVISION exhibited a pronounced nonlinear positive relationship with SHAP values, broadly resembling the response patterns observed in spring and autumn. When DIVISION was below approximately 0.40, SHAP values were predominantly negative. As DIVISION increased beyond approximately 0.45, SHAP values gradually

became positive and reached relatively high levels within the range of 0.80–0.90. LPI displayed a distinct non-monotonic response pattern. At low LPI values, its SHAP contributions were strongly positive, but progressively declined and generally became negative around 35–40. A moderate rebound in SHAP values occurred within the range of 65–85, followed by a sharp decline when LPI exceeded approximately 90. PD generally exhibited a sustained negative relationship with SHAP values, with its negative contribution becoming increasingly pronounced as PD increased, particularly beyond approximately 10.

Taken together, the SHAP dependence plots reveal substantial seasonal differences in the nonlinear contributions of forest landscape metrics to predicted LST. Among the metrics examined, DIVISION exhibited a relatively consistent nonlinear positive response across all four seasons, indicating comparatively stable cross-seasonal contribution characteristics. By contrast, LPI showed stronger seasonal variability in its response patterns, exhibiting a predominantly monotonic negative relationship in summer but more complex non-monotonic relationships in autumn and winter. PD generally displayed negative response patterns in autumn and winter, whereas MPA made a relatively pronounced negative contribution in summer. These findings demonstrate that the relationships between forest landscape patterns and LST cannot be adequately characterized by simple linear associations. Instead, the direction and magnitude of metric contributions, together with their potential transition points, vary across seasons, highlighting the seasonal complexity of the relationships between forest landscape configuration and the surface thermal environment.

4. Discussion

4.1. Seasonal Differences in the Relationship Between Forest Landscape Patterns and LST

This study revealed pronounced seasonal variations in the relationships between forest landscape patterns and LST in Ningbo, indicating that the association between forest landscapes and the urban thermal environment is determined not solely by forest cover but also by spatial configuration and seasonally varying environmental conditions. Seasonal differences in vegetation physiological activity, radiation regimes, and surface energy exchange processes may further modulate these relationships [32,33]. Consequently, assessments based on annual mean LST or observations from a single season may fail to capture the seasonal heterogeneity of forest-related thermal patterns. By developing independent models for each of the four seasons, this study provides further insights into the season-specific relationships between forest landscape patterns and the urban thermal environment.

The relative contributions of individual landscape metrics also varied across seasons. LPI made a greater contribution to model predictions in spring and summer, whereas DIVISION was more influential in autumn and winter. This seasonal shift suggests that the relative importance of dominant forest patch size and landscape fragmentation in explaining spatial variations in LST is season dependent. Accordingly, assessments of the thermal regulation potential of urban forests should extend beyond forest cover and incorporate multiple dimensions of landscape structure, particularly dominant patch size, the degree of spatial fragmentation, and their season-specific relationships with LST.

4.2. Nonlinear Responses of Forest Landscape Metrics and Implications for Urban Planning

Both LPI and DIVISION exhibited high importance across the four seasonal models, indicating that they are key landscape metrics for explaining spatial variations in seasonal LST. LPI characterizes the relative dominance of the largest forest patch within the landscape. A higher LPI generally indicates a larger proportion of the landscape occupied by the dominant forest patch, which may help maintain canopy continuity and enhance

shading and evapotranspiration [34,35]. In this study, LPI generally showed predominantly negative SHAP values, suggesting that larger dominant forest patches were associated with lower model-predicted LST. This finding highlights the importance of considering not only the overall extent of urban forests but also the preservation of large, dominant patches and their spatial integrity in urban forest planning.

In contrast, DIVISION exhibited an overall positive nonlinear response across the four seasons, suggesting that greater landscape fragmentation was generally associated with higher model predicted LST. Increased fragmentation may weaken the spatial continuity of forest patches, increase the interfaces between forested and non-forested surfaces, and expose individual forest patches to greater influences from surrounding land cover types [36,37]. These findings indicate that patch dominance and landscape fragmentation represent distinct dimensions of forest spatial structure. Consequently, even landscapes with comparable forest coverage may exhibit different contributions to LST predictions because of differences in their spatial configurations.

The SHAP dependence plots further revealed season nonlinear response patterns among the key landscape metrics. DIVISION exhibited an overall positive response in all four seasons, although the magnitude and shape of the response, as well as the potential transition points, varied seasonally. LPI showed a predominantly monotonic negative response in summer but exhibited non-monotonic patterns in autumn and winter, suggesting that its relationship with LST may vary with other landscape characteristics and seasonal environmental conditions. In addition, PD generally showed a negative response in autumn and winter, whereas MPA exhibited a relatively pronounced negative SHAP contribution in summer, with different response directions observed in other seasons. These findings suggest that forest landscape optimization should not rely on a single metric but should account for multiple dimensions of patch structure and spatial configuration in consideration of seasonal variations. From a planning perspective, priority should be given to conserving large, dominant forest patches and improving spatial connectivity in highly fragmented areas to enhance overall landscape continuity [38,39]. Nevertheless, the values at which SHAP contributions change from positive to negative should be interpreted as potential response transition points rather than ecologically established thresholds. They have not been independently validated through statistical threshold analysis and should therefore not be directly adopted as quantitative planning standards.

Methodologically, this study integrated the Extra Trees algorithm with SHAP to capture nonlinear relationships between forest landscape metrics and LST while quantifying the relative importance and direction of individual feature contributions to model predictions. This framework helps address the limitations of conventional linear approaches in characterizing complex response relationships and improves the interpretability of machine-learning results. Nevertheless, SHAP values quantify the contributions of individual features to model predictions rather than their independent causal effects [40]. Therefore, the identified relationships should be interpreted as model-based associations, and further investigation incorporating additional environmental variables and causal inference approaches is needed to clarify the underlying mechanisms.

4.3. Limitations and Future Research

This study has several limitations that should be addressed in future research. First, the seasonal LST dataset was derived from Landsat 8 imagery acquired in 2025. Data from a single year are insufficient to capture long-term climatic variability or fully characterize how the relationships between forest landscape patterns and LST may change under extreme heat conditions. Future studies should incorporate multi-year and multi-temporal remote sensing observations to assess the interannual stability of the relationships between key landscape metrics and LST, as well as their responses to heatwave events.

Second, this study primarily used seven forest landscape metrics as model predictors without systematically incorporating other potentially influential factors, including elevation, slope, impervious surface proportion, building morphology, distance from the coastline, and meteorological conditions. Given Ningbo's diverse geographical setting, which encompasses coastal plains, densely built-up urban areas, and mountainous terrain, these factors may jointly influence LST and modify the relative contributions of forest landscape metrics to model predictions. Accordingly, the findings should be interpreted as model-based associations between forest landscape patterns and LST, rather than as independent effects isolated from other environmental influences. Future research should integrate topographic, built environment, land cover, and meteorological variables to better account for potential environmental confounding factors. Third, this study adopted a regular grid with a spatial resolution of 600 × 600 m as the analytical unit. Different spatial resolutions may produce different statistical relationships between landscape metrics and LST because of scale-dependent effects. Future studies could combine multiscale grid analysis with moving window approaches to investigate the scale dependence of these relationships. In addition, spatial autocorrelation among grid cells may compromise the independence of model samples. Although this study employed a random partition of the training and testing datasets, this approach cannot fully eliminate the risk of spatial information leakage and may overestimate model generalization performance. Spatial block cross-validation and validation using independent regional datasets could therefore be adopted in future research to provide a more rigorous assessment of spatial transferability. Finally, remotely sensed LST characterizes the thermal state of the land surface and does not directly represent near surface air temperature or human thermal comfort. Future investigations should integrate ground meteorological observations, microclimate measurements, evapotranspiration data, and thermal comfort indices to provide a more comprehensive assessment of the relationships between forest landscape structure and the urban thermal environment. Furthermore, segmented regression and causal inference approaches could be employed to identify and validate potential response thresholds and clarify their ecological significance.

5. Conclusions

Taking Ningbo City as the study area, this study integrated Landsat 8 remote sensing imagery, the CLCD, the Extra Trees algorithm, and SHAP analysis to systematically investigate the relationships between forest landscape patterns and seasonal LST. Specifically, this study aimed to quantify the relative contributions of different forest landscape metrics, characterize their contribution directions and nonlinear response patterns, and examine seasonal variations in the associations between forest landscape structure and the surface thermal environment.

The results revealed pronounced seasonal variations and spatial heterogeneity in LST across Ningbo, with the highest temperatures occurring in summer and the lowest in winter. The Extra Trees model effectively captured the relationships between forest landscape metrics and seasonal LST, although its predictive performance varied across seasons. SHAP analysis identified the LPI and DIVISION as the two most influential metrics across all four seasonal models. The relative contribution of LPI was greater in spring and summer, whereas DIVISION was more influential in autumn and winter. These findings highlight the seasonal dependence of the relationships between forest landscape patterns and the surface thermal environment.

The nonlinear response analysis further revealed distinct response patterns among individual landscape metrics. LPI generally exhibited negative SHAP contributions, although its response patterns differed across seasons. Specifically, LPI showed a predominantly monotonic negative response in summer but exhibited more complex, non-

monotonic patterns in autumn and winter. In contrast, DIVISION displayed an overall positive nonlinear response across all four seasons, suggesting that greater forest landscape fragmentation was generally associated with higher model predicted LST. Moreover, the contribution directions and magnitudes of other metrics, particularly PD and MPA, also varied seasonally. Collectively, these findings indicate that the association between forest landscape patterns and LST is related not only to the dominance of large forest patches but also to landscape fragmentation and its season specific response patterns, providing further insight into the complex relationships between urban forest spatial configuration and the surface thermal environment.

Theoretically, this study elucidates the nonlinear and seasonally heterogeneous relationships between forest landscape patterns and LST, providing empirical evidence for understanding how urban forest spatial structure is associated with variations in the surface thermal environment. Methodologically, the integration of Extra Trees and SHAP establishes an analytical framework that combines nonlinear relationship modeling with model interpretability. This framework provides an effective approach for identifying influential landscape metrics, quantifying their contributions to model predictions, and exploring potential response transition points. From a practical perspective, the findings suggest that urban forest planning should extend beyond the consideration of overall forest coverage to emphasize the conservation of large, dominant forest patches and the mitigation of excessive landscape fragmentation. Such strategies may help improve forest landscape continuity and optimize urban forest spatial configuration, thereby contributing to urban thermal environment improvement. This study extends the investigation of urban forest landscape patterns and the surface thermal environment to a seasonal perspective, providing quantitative evidence and scientific insights for urban forest spatial planning and seasonally informed thermal environment management.

Author Contributions: Conceptualization, Y.Z.; data curation, H.Z.; Methodology, L.Z.; visualization, L.Z.; writing—original draft, L.Z.; writing—review and editing, H.Y. H.Y. is responsible for future questions from readers as the corresponding author. All authors have read and agreed to the published version of the manuscript.

Funding: This research is funded by Zhejiang Key Laboratory of Film and TV Media Technology; Zhejiang Engineering Research Center of Intelligent Media; and National Radio and Television Administration Laboratory for Media Intelligent Communication Technology.

Data Availability Statement: The data are not publicly available due to privacy. The data presented in this paper are available on request from the corresponding author.

Conflicts of Interest: The authors declare no conflicts of interest.

References

1. Ji, Y.; Peng, Y.; Li, Z.; Li, J.; Liu, S.; Cai, X.; Yin, Y.; Feng, T. Driving Mechanism of Differentiation in Urban Thermal Environment during Rapid Urbanization. *Remote Sens.* **2023**, *15*, 2075.
2. Kecman, S.; Stojanović, N.; Vukmirović, M.; Vasiljević, N.; Bjedov, I.; Vujović, D. The Impact of the Small Urban Green Space on the Urban Thermal Environment: The Belgrade Case Study (Serbia). *Forests* **2025**, *16*, 321.
3. Qian, Z.; Sun, Y.; Chen, Z.; Ji, F.; Feng, G.; Ma, Q. Analysis of Land Surface Temperature Sensitivity to Vegetation in China. *Remote Sens.* **2023**, *15*, 4544.
4. Fang, R.; Shan, X.; Deng, Q. Research on Air Temperature Inversion Method Based on Land Surface Temperature of Different Land Surface Cover. *Atmosphere* **2025**, *16*, 754.
5. Li, Y.; Liu, S.; Liu, M.; Guo, R.; Shi, Y.; Peng, X.; Feng, S. Evolution and Built-Up Age Dependency of Urban Thermal Environment. *Remote Sens.* **2024**, *16*, 1495.
6. Kang, X.; Yang, J.; Zhang, Y.; Zou, Q.; Li, Z.; Feng, Y.; Xiao, X.; Xia, J. Effects of urban forest structure on land surface temperature: Subtropical versus temperate cities. *Urban For. Urban Green.* **2026**, *120*, 129423.

7. Shen, W.; Liu, Q.; Ji, M.; He, J.; He, T.; Huang, C. Impacts of urban forests and landscape characteristics on land surface temperature in two urban agglomeration areas of China. *Sustain. Cities Soc.* **2023**, *90*, 104909.
8. Zhang, Z.; Yang, K.; Wang, L.; Cheng, K.; Chen, C.; Ding, C. Regulation effect of planted forests on land surface temperature in China. *Agric. For. Meteorol.* **2025**, *372*, 110660.
9. Rosas-Chavoya, M.; López-Serrano, P.M.; Vega-Nieva, D.J.; Hernández-Díaz, J.C.; Wehenkel, C.; Corral-Rivas, J.J. Estimating Above-Ground Biomass from Land Surface Temperature and Evapotranspiration Data at the Temperate Forests of Durango, Mexico. *Forests* **2023**, *14*, 299.
10. Wang, N.; Li, L.; Jin, S.; Zhao, L. The Mitigating Effect of Urban Forest Landscape Structure on Urban Heat Islands: Nonlinear Response and Interaction Effect. *Forests* **2026**, *17*, 694.
11. Wang, X.; Chen, Y.; Wang, Z.; Xu, B.; Feng, Z. Multi-Temporal Analysis of the Impact of Summer Forest Dynamics on Urban Heat Island Effect in Yan'an City. *Sustainability* **2024**, *16*, 3473.
12. Lin, L.; Bai, G.; Han, T. Assessing the Relationship Between Seasonal Urban Heat Island Effects and Forest Structure in Hangzhou City Using the XGBoost Model. *Forests* **2026**, *17*, 545.
13. Yu, Y.; Li, Y.; Liu, Y.; Liu, D.; Chen, H.; Zhao, Z. Asymmetry of Land Surface Temperature Response to Forest Gain and Loss: The Role of Land Cover Conversions. *Geophys. Res. Lett.* **2026**, *53*, e2026GL123073.
14. Zhang, Y.; Luo, Y.; Han, L.; Chen, K.; Wang, Z.; Yang, Q. Importance of Patches in Maintaining Forest Landscape Connectivity: A Case Study of Barluk, Xinjiang, China. *Forests* **2025**, *16*, 74.
15. He, Z.; Lin, Z.; Xu, Q.; Ding, S.; Bao, X.; Li, X.; Hu, X.; Li, J. Multi-Dimensional Landscape Connectivity Index for Prioritizing Forest Cover Change Scenarios: A Case Study of Southeast China. *Forests* **2024**, *15*, 1490.
16. Hou, F.; Taib, N.; Marzbali, M.; Abdullah, A. Revealing the synergistic effects of built-up space and green space morphology in mitigating seasonal daytime and nighttime land surface temperatures in Shanghai. *J. Environ. Manag.* **2026**, *415*, 130576.
17. Liao, Z.; Zhang, C.; Wang, Y.; Wu, J.; Yan, W.; Su, Y. Biodiversity regulates the asymmetric influence of forest cover gain and loss on land surface temperature. *Commun. Earth Environ.* **2025**, *7*, 19.
18. Guan, S.; Liu, S.; Zhang, X.; Du, X.; Lv, Z.; Hu, H. Analysis of Supply–Demand Relationship of Cooling Capacity of Blue–Green Landscape under the Direction of Mitigating Urban Heat Island. *Sustainability* **2023**, *15*, 10919.
19. Sánchez-Sánchez, F.A.; Vega-De-Lille, M.; Castillo-Atoche, A.A.; López-Maldonado, J.T.; Cruz-Fernandez, M.; Camacho-Pérez, E.; Rodríguez-Reséndiz, J. Geo-Sensing-Based Analysis of Urban Heat Island in the Metropolitan Area of Merida, Mexico. *Sensors* **2024**, *24*, 6289.
20. Tanoori, G.; Soltani, A.; Modiri, A. Machine Learning for Urban Heat Island (UHI) Analysis: Predicting Land Surface Temperature (LST) in Urban Environments. *Urban Clim.* **2024**, *55*, 101962.
21. Hou, X.; Xie, X.; Bagan, H.; Chen, C.; Wang, Q.; Yoshida, T. Exploring Spatiotemporal Variations in Land Surface Temperature Based on Local Climate Zones in Shanghai from 2008 to 2020. *Remote Sens*. **2023**, *15*, 3106.
22. Wang, S.; Liu, Y.; Guo, J.; Liu, J.; Chai, H. Impacts of the Middle Route of the South-to-North Water Diversion Project on Land Surface Temperature and Fractional Vegetation Coverage in the Danjiang River Basin. *Remote Sens*. **2024**, *16*, 2665.
23. Azimi, H.; Shiri, H. Extra Tree Regression Algorithm for Simulation of Iceberg Draft and Subgouge Soil Characteristics. *Water* **2025**, *17*, 2425.
24. Hong, T.; Yim, S.H.L.; Heo, Y. Interpreting complex relationships between urban and meteorological factors and street-level urban heat islands: Application of random forest and SHAP method. *Sustain. Cities Soc*. **2025**, *126*, 106353.
25. Ma, K.; Jiang, C.; Long, Y.; Wu, Z.; Yan, S. Enhanced Runoff Prediction in Zijiang River Basin Using Machine Learning and SHAP-Based Interpretability. *Water* **2026**, *18*, 601.
26. Bovkir Tonbul, R. Understanding Land Surface Temperature Patterns in Istanbul: The Role of Blue–Green and Built-Environment Predictors Using Explainable Machine Learning. *ISPRS Int. J. Geo-Inf*. **2026**, *15*, 455.
27. He, R.; Wang, J.; Liu, D. Multi-Scale Effects of 2D/3D Urban Morphology Factors on Land Surface Temperature Using LightGBM-SHAP: A Case Study in Beijing. *Remote Sens*. **2026**, *18*, 1287.
28. Stamou, A.; Karachaliou, E.; Tavantzis, I.; Stylianidis, E. Decoding Urban Heat Dynamics: The Role of Morphological and Structural Parameters in Shaping Land Surface Temperature from Satellite Imagery. *ISPRS Int. J. Geo-Inf*. **2026**, *15*, 174.
29. Šamanović, S.; Bjelotomić Oršulić, O.; Cetl, V.; Krtalić, A. The Influence of Three-Dimensional Urban Form on the Dynamics of Urban Thermal Patterns: A Case Study of Zagreb, Croatia. *Land* **2026**, *15*, 693.
30. Omoniyi, T.O.; Sims, A.; McRoberts, R.E. Estimating Forest Volume and Forest Volume Change Using Random Forests and Sentinel-2 Data. *Remote Sens*. **2026**, *18*, 2134.

31. Chi, D.; Wang, Z.; Liu, H. A Multivariate Linear Regression-Based Ultrasonic Non-Destructive Evaluating Method for Characterizing Weld Tensile Strength Properties. *Materials* **2025**, *18*, 1925.
32. Pinagé, E.R.; Bell, D.M.; Longo, M.; Silva, C.A.; Csillik, O.; Huete, A. Surface energy dynamics and canopy structural properties in intact and disturbed forests in the Southern Amazon. *J. Geophys. Res. Biogeosci.* **2023**, *128*, e2023JG007465.
33. Qu, Z.; Li, X.; Shi, F. Contrasting Responses of Land Surface Temperature and Soil Temperature to Forest Expansion During the Dormant Season on the Qinghai-Tibet Plateau. *J. Geophys. Res. Atmos*. **2024**, *129*, e2023JD039595.
34. Zhou, W.; Cao, F.; Wang, G. Effects of Spatial Pattern of Forest Vegetation on Urban Cooling in a Compact Megacity. *Forests* **2019**, *10*, 282.
35. Song, Y.; Song, X.; Shao, G. Effects of Green Space Patterns on Urban Thermal Environment at Multiple Spatial–Temporal Scales. *Sustainability* **2020**, *12*, 6850.
36. Ma, J.; Li, J.; Wu, W.; Liu, J. Global Forest Fragmentation Change from 2000 to 2020. *Nat. Commun.* **2023**, **14**, 3752.
37. Lin, X.; Zhen, S.; Zhao, Q.; Hu, X. A New Paradigm for Assessing Detailed Dynamics of Forest Landscape Fragmentation. *Forests* **2024**, *15*, 1212.
38. Jin, L.; Song, Y. Forest Landscape Connectivity to Prioritize Afforestation in Urban Ecosystems: Seoul as a Case Study. *Urban For. Urban Green.* **2023**, *90*, 128122.
39. Beltrão, M.G.; Gonçalves, C.F.; Brancalion, P.H.S.; Carmignotto, A.P.; Silveira, L.F.; Galetti, P.M., Jr.; Galetti, M. Priority Areas and Implementation of Ecological Corridor through Forest Restoration to Safeguard Biodiversity. *Sci. Rep*. **2024**, *14*, 30837.
40. Chen, H.; Lundberg, S.M.; Lee, S.-I. Explaining a Series of Models by Propagating Shapley Values. *Nat. Commun*. **2022**, *13*, 4512.

Disclaimer/Publisher's Note: The statements, opinions and data contained in all publications are solely those of the individual author(s) and contributor(s) and not of MDPI and/or the editor(s). MDPI and/or the editor(s) disclaim responsibility for any injury to people or property resulting from any ideas, methods, instructions or products referred to in the content.